HIV

# The receptor repertoire and functional profile of follicular T cells in HIV-infected lymph nodes



**Ben S. Wendel,[1]* Daniel del Alcazar,[2,3]* Chenfeng He,[4]* Perla M. Del Río-Estrada,[5] Benjamas Aiamkitsumrit,[2,3] Yuria Ablanedo-Terrazas,[5] Stefany M. Hernandez,[1] Ke-Yue Ma,[6] Michael R. Betts,[7] Laura Pulido,[8] Jun Huang,[8] Phyllis A. Gimotty,[9] Gustavo Reyes-Terán,[5] Ning Jiang,[4,6†] Laura F. Su[2,3†]**

**Follicular helper CD4$^+$ T cells ($T_{FH}$) play an integral role in promoting B cell differentiation and affinity maturation. Whereas $T_{FH}$ cell frequencies are increased in lymph nodes (LNs) from individuals infected with HIV, humoral immunity remains impaired during chronic HIV infection. Whether HIV inhibits $T_{FH}$ responses in LNs remains unclear. Advances in this area have been limited by the difficulty of accessing human lymphoid tissues. Here, we combined high-dimensional mass cytometry with T cell receptor repertoire sequencing to interrogate the composition of $T_{FH}$ cells in primary human LNs. We found evidence for intact antigen-driven clonal expansion of $T_{FH}$ cells and selective utilization of specific complementarity-determining region 3 (CDR3) motifs during chronic HIV infection, but the resulting $T_{FH}$ cells acquired an activation-related $T_{FH}$ cell signature characterized by interleukin-21 (IL-21) dominance. These IL-21$^+$ $T_{FH}$ cells contained an oligoclonal HIV-reactive population that preferentially accumulated in patients with severe HIV infection and was associated with aberrant B cell distribution in the same LN. These data indicate that $T_{FH}$ cells remain capable of responding to HIV antigens during chronic HIV infection but become functionally skewed and oligoclonally restricted under persistent antigen stimulation.**

## INTRODUCTION

Follicular helper T cells ($T_{FH}$) provide key signals necessary for B cell recruitment and selection to generate protective antibody responses (*1*, *2*). During untreated chronic HIV infection, $T_{FH}$ cells become highly expanded in the lymph nodes (LNs) (*3*, *4*). Despite this, HIV$^+$ patients generate diminished protective antibody responses against immune challenges. For example, HIV-infected individuals produce lower titers of antibodies and less durable responses to seasonal influenza vaccines (*5*, *6*). The prevailing model suggests that $T_{FH}$ cells from HIV patients are ineffective at providing B cell help based on in vitro assays that showed less robust antibody production by B cells cocultured with $T_{FH}$ cells from HIV$^+$ patients (*7*–*9*). A proposed mechanism for this involves up-regulation of programmed cell death–ligand 1 (PD-L1) by B cells, which interacts with programmed cell death–1 (PD-1) on $T_{FH}$ cells to inhibit T cell receptor (TCR)–dependent activation of $T_{FH}$ cells (*7*). However, the extent to which $T_{FH}$ cells express impaired antigen responsiveness in vivo remains unclear. Because $T_{FH}$ cells need to appropriately sense antigen signals to discriminate between B cells, defective response to antigen not only impairs provision of T cell help to individual B cells but also imperils the process of B cell selection on a global level.

Here, we interrogated the functional phenotype and TCR repertoire composition of primary $T_{FH}$ cells isolated directly from LNs from HIV$^+$ individuals. We used the presence or absence of antigen-dependent TCR signatures to address the responsiveness of $T_{FH}$ cells to antigen engagement and applied high-dimensional mass cytometry to elucidate how HIV infection alters the functional phenotype of $T_{FH}$ cells in the lymphoid compartment. Our data revealed clonal expansion and convergent selection for Gag-reactive TCRs in $T_{FH}$ cells in the germinal centers (GCs) of HIV-infected LNs, indicating that $T_{FH}$ cells remain capable of responding to HIV antigens during chronic HIV infection. However, $T_{FH}$ cells in LNs from HIV$^+$ individuals acquire an activated phenotype dominated by interleukin-21 (IL-21) production, which were less polyfunctional and correlated with aberrant changes in B cell development. By combining antigen-specific analyses with single-cell TCR sequencing, we further demonstrated that IL-21$^+$ $T_{FH}$ cells contained an HIV-reactive population expressing a restricted TCR repertoire and GC phenotype. Thus, TCR-directed response to HIV alters $T_{FH}$ cell diversity and composition in the lymphoid compartment.

## RESULTS

### HIV-infected LNs contain clonally expanded GC $T_{FH}$ cells

LNs from untreated HIV$^+$ patients contain a high frequency of $T_{FH}$ cells, but the mechanism that drives expansion of $T_{FH}$ cells remains unclear. The enrichment of HIV antigens (*10*, *11*) and the highly proinflammatory milieu (*12*, *13*) in the LNs could lead to antigen-driven and/or bystander T cell expansion. To address whether proliferation of $T_{FH}$ cells is antigen-dependent, we tested whether HIV induces selective proliferation of certain T cell clones. We focused on GC $T_{FH}$ cells because the frequency of these cells becomes greatly increased during chronic HIV infection (*3*, *4*). To identify GC $T_{FH}$

[1]McKetta Department of Chemical Engineering, Cockrell School of Engineering, University of Texas at Austin, Austin, TX 78712, USA. [2]Department of Medicine, Perelman School of Medicine, University of Pennsylvania and Philadelphia Veterans Affairs Medical Center, Philadelphia, PA 19104, USA. [3]Institute for Immunology, Perelman School of Medicine, University of Pennsylvania, Philadelphia, PA 19104, USA. [4]Department of Biomedical Engineering, Cockrell School of Engineering, University of Texas at Austin, Austin, TX 78712, USA. [5]Departamento de Investigación en Enfermedades Infecciosas, Instituto Nacional de Enfermedades Respiratorias, Ciudad de México, México. [6]Institute for Cellular and Molecular Biology, College of Natural Sciences, University of Texas at Austin, Austin, TX 78712, USA. [7]Department of Microbiology and Institute for Immunology, Perelman School of Medicine, University of Pennsylvania, Philadelphia, PA 19104, USA. [8]Institute for Molecular Engineering, University of Chicago, Chicago, IL 60637, USA. [9]Department of Biostatistics, Epidemiology and Informatics, Perelman School of Medicine, University of Pennsylvania, Philadelphia, PA 19104, USA.
*These authors contributed equally to this work.
†Corresponding author. Email: laurasu@upenn.edu (L.F.S.); jiang@austin.utexas.edu (N.J.)

cells, we selected memory CD4$^+$ T cells that express $T_{FH}$ cell markers CXCR5 and PD-1. CD57 is a glycan carbohydrate epitope expressed by $T_{FH}$ cells in the GC, and we used this marker to further demarcate the GC subset (*14*–*17*). Naïve CD4$^+$ T cells were identified by CD45RO$^-$CXCR5$^-$CD57$^-$CCR7$^+$ expression, and memory CD4$^+$ T cells were identified by CD45RO$^+$CXCR5$^-$ staining and excluded for PD-1 and inducible T cell costimulator (ICOS)–positive cells (Fig. 1A). We sorted 1464 to 15,000 naïve, memory, and GC $T_{FH}$ cells from freshly thawed LN samples and analyzed the TCR sequences of these subsets using a molecular identifier (MID)–based approach to increase the accuracy of repertoire sequencing (table S1) (*18*, *19*). Because the variability of TCR sequences is encoded in the complementarity-determining region 3 (CDR3) region, we used the number of transcripts detected for a particular CDR3 sequence to define TCR clone size. On average, 11,839 TCR transcripts were detected for each sample (table S2). Unique TCR frequencies range from 1 in 37,129 (0.003%) for the rarest clones to 250 in 2498 (~10%) for the most expanded clone. To compare the degree of relative clonal expansion, we categorized TCR frequency into six groups, ranging from rare (<0.1%) to >2%, according to the clone size relative to the total TCR transcripts detected in that sample. As expected, the TCR repertoire of naïve CD4$^+$ T cells was composed mostly of rare clones. In contrast, the TCR repertoire of GC $T_{FH}$ cells had a much higher fraction of TCRs occupied by abundant clones (>0.1%) compared with naïve and memory CD4$^+$ T cells (Fig. 1B and fig. S1). The degree of TCR clonal expansion was quantified by normalized Shannon entropy (NSE) (*20*, *21*). Consistent with the hypothesis that the increase in GC $T_{FH}$ cell frequency is due to selective proliferation of certain T cell clones, GC $T_{FH}$ cells had a lower NSE score compared with naïve and memory cells (Fig. 1C). Together, our data demonstrated a notable expansion of clone size in GC $T_{FH}$ cell populations.

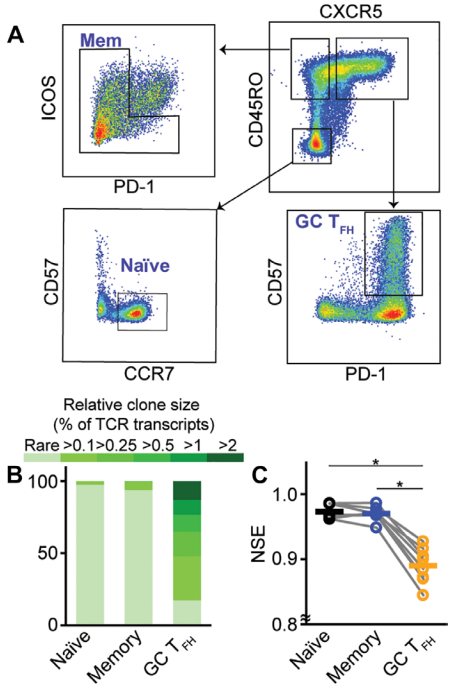


**Fig. 1. GC $T_{FH}$ cells become clonally expanded.** (**A**) Representative plots showing sorting strategy to identify naïve, memory, and GC $T_{FH}$ cells. (**B**) Breakdown of the proportion of the TCR repertoire represented by clones of different sizes for sorted naïve, memory, and GC $T_{FH}$ cells from HIV$^+$ LNs. TCR clone size was normalized by the total number of TCR transcripts on nucleotide sequences. (**C**) NSE of the TCR repertoire of sorted naïve, memory, and GC $T_{FH}$ cells. Gray lines link the same patient. Bars indicate means. *$P < 0.05$ by two-tailed Wilcoxon signed-rank test ($n = 8$ HIV-infected LNs).

## TCRs from GC $T_{FH}$ cells exhibit signatures of antigen-driven clonal convergence

Next, to test whether clonal expansion in GC $T_{FH}$ cells from HIV-infected LNs was antigen-driven, we analyzed the TCR sequences for evidence of convergence to the same amino acid sequence from distinct nucleotide sequences. Unlike B cells, which can undergo somatic hypermutation, the TCR sequence of a naïve T cell is determined during maturation in the thymus and remains fixed throughout the life spans of the T cell and its progeny. Thus, with the exception of clones that express two TCRα or TCRβ sequences, distinct TCR nucleotide sequences necessarily arise from distinct naïve T cells. However, multiple nucleotide sequences of different TCRs may encode the same amino acid sequence. These degenerate TCR sequences are typically rare, and the presence of these sequences suggests antigen selection pressure that favors certain TCR motifs that recognize particular antigen(s). Thus, having highly abundant CDR3 amino acid sequences that are encoded by multiple distinct nucleotide sequences indicates preferential expansion of T cells with that specificity (*20*). On the other hand, we would not expect multiple nucleotide sequences to converge on the amino acid level in the absence of strong antigen-driven selection. Following this logic, we translated the TCR nucleotide sequences into amino acid sequences and tallied the number of different nucleotide sequences that encode each CDR3 amino acid sequence. These CDR3 amino acid sequences can be broken into four quadrants—Q1, Q2, Q3, and Q4—based on the level of degeneracy and frequency in the repertoire (Fig. 2A and fig. S2). Q1 contains highly expanded amino acid CDR3 sequences that are encoded by two or more nucleotide sequences (Fig. 2B). These degenerate, abundant clones likely arose from strong antigen-driven selection and proliferation. Q2 contains low-frequency amino acid CDR3 sequences that are also encoded by two or more nucleotide sequences. Degenerate clones can stochastically arise in the repertoire, but these are typically rare as reflected by the low frequency of nonclonally expanded sequences in Q2. Q3 contains amino acid CDR3 sequences that show neither clonal expansion nor amino acid convergence and make up most of the repertoire. Q4 contains expanded amino acid CDR3 sequences derived from a single nucleotide sequence and are therefore nondegenerate. This TCR degeneracy analysis revealed a significantly higher degree of antigen-driven clonal convergence in GC $T_{FH}$ cells compared with naïve and memory T cells (Fig. 2C). Together with the NSE decrease in GC $T_{FH}$ cells, these data provide further evidence that antigen-driven clonal expansion is preserved in GC $T_{FH}$ cells.

## HIV promotes selective expansion of HIV-reactive $T_{FH}$ cells

To determine whether clonally expanded and/or convergently selected TCRs include HIV-specific sequences, about 2 to 3 million thawed LN cells were cultured with an HIV-1 consensus B Gag peptide pool for 3 to 4 weeks and then restimulated with the same peptide pool for 4 hours to identify antigen-specific T cells by CD40L and CD69 up-regulation (fig. S3). LN cells were also stimulated with an overlapping set of hemagglutinin (HA) peptides from influenza virus (A/California/7/2009) as a non-HIV control. TCRs from CD40L$^+$CD69$^+$ Gag- or HA-reactive T cells were used to generate a reference TCR panel (table S3). These antigen-specific TCR sequences were mapped onto our bulk T cell sequencing data from freshly thawed LN cells

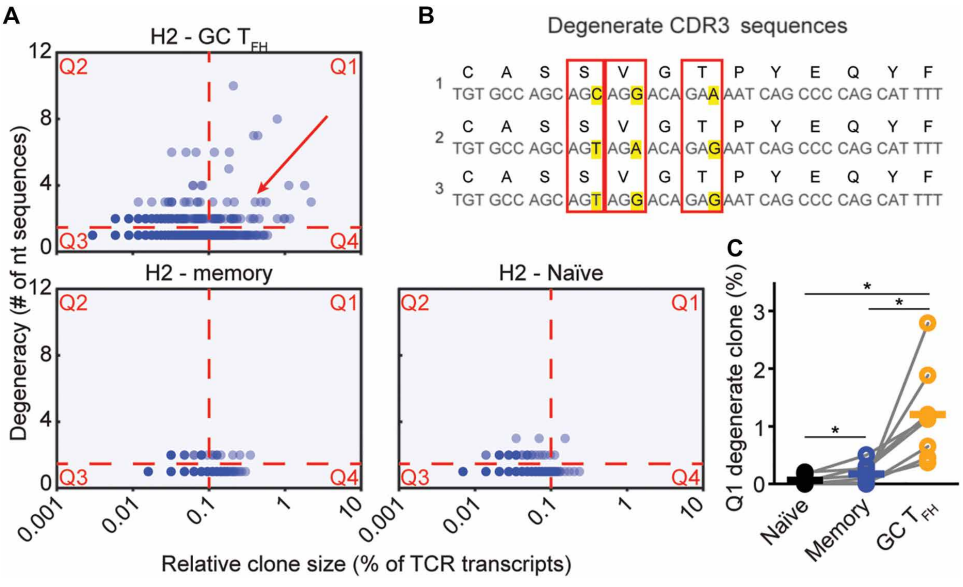


**Fig. 2. Antigen-driven clonal selection signature in GC $T_{FH}$ cells of HIV-infected LNs.** (**A**) Representative degeneracy plot from sample H2. Coding degeneracy level [number of unique TCR nucleotide (nt) sequences encoding a common CDR3 amino acid sequence] of each CDR3 amino acid sequence is plotted against their frequency (measured as percentage of total TCR transcripts) in naïve, memory, and GC $T_{FH}$ cells. Each dot is a unique CDR3 amino acid sequence. Red dashed lines indicate cutoffs for degenerate (two or more nucleotide sequences coding for the same amino acid sequence; horizontal) and expanded (0.1% or more of TCR transcripts; vertical) clones. Red arrow points to example degenerate clone in (B). (**B**) Example of CDR3 amino acid degeneracy. Amino acid (top row) and nucleotide (bottom row) sequences for three distinct nucleotide sequences (0.41% of total TCR transcripts) that code for the same amino acid sequence as indicated by arrow in (A): $Y = 3$ and $X = 0.41\%$. Red boxes and highlights indicate redundant codons. (**C**) Comparison of Q1 degenerate-abundant clone percentage in naïve, memory, and GC $T_{FH}$ cells. Gray lines link the same patient. Bars indicate means. *$P < 0.05$ by two-tailed Wilcoxon signed-rank test ($n = 8$ HIV-infected LNs).

to determine which sequences were Gag- or HA-specific. Common sequences shared between naïve, memory, or GC $T_{FH}$ cells were shown as connecting lines on circos plots (Fig. 3A).

We found several Gag-specific TCR sequences in the GC $T_{FH}$ (zero to seven clones) population. Although we did not have enough data points to reach significance, the overlap between Gag-specific TCR sequences was minimal in memory T cells (zero or one clone), and no Gag-specific sequences were found in the naïve T cell population (Fig. 3B). A similar trend of enrichment of antigen-specific clones in the GC $T_{FH}$ cells was also observed for HA-specific TCR sequences (fig. S4). This is unsurprising because these individuals have likely been exposed to influenza infection and/or vaccinated against HA in the past. However, analysis of combined TCR sequencing data from all individuals showed that these Gag-specific GC $T_{FH}$ cells, but not the HA-specific clones, were highly expanded compared with the bulk GC $T_{FH}$ cells of unknown specificity (Fig. 3C). Translating these antigen-specific TCR sequences into amino acid sequences showed that the Gag-specific TCR sequences within the GC $T_{FH}$ population, but not the HA-specific sequences, have a significantly higher degree of coding degeneracy (Fig. 3D). Thus, the Gag-specific GC $T_{FH}$ cells were preferentially expanded and degenerate. Collectively, these data indicate that Gag-specific $T_{FH}$ cells respond to antigen stimulation and become selectively expanded in the LNs.

## $T_{FH}$ cells acquire distinct phenotypic characteristics in HIV-infected LNs

To investigate HIV-driven changes on the phenotypic level, we designed a mass cytometry panel to examine phenotypic and functional features of $T_{FH}$ cells (table S4). Cryopreserved cervical LNs from 25 Mexican HIV$^+$ patients were obtained and analyzed together with cervical, mesenteric, and iliac LNs from seven local healthy controls (HCs) (table S5). To interrogate the functional potential of $T_{FH}$ cells, 3 to 5 million cryopreserved LN cells were thawed and stimulated with phorbol 12-myristate 13-acetate (PMA) and ionomycin in the presence of brefeldin A and monensin for 5 hours. Cells were then stained with metal-conjugated antibodies and acquired on the CyTOF 2 mass cytometer. Bead-based standards were used to correct for machine performance and batch differences (fig. S5) (*22*). To broadly define CD4$^+$ T cells with $T_{FH}$ cell features, we performed manual gating to select CD4$^+$ T cells positive for CXCR5 and CD45RO staining. GC $T_{FH}$ cells were further identified by PD-1 and CD57 expression and imported into Cytobank (Fig. 4A and fig. S6). T-distributed stochastic neighbor embedding (t-SNE) was performed using the viSNE implementation to create two-dimensional plots that placed cells with similar phenotypic characteristics in close proximity.

We used contour maps to facilitate visualization of cellular distribution, which showed a different pattern between GC $T_{FH}$ cells from HC and HIV$^+$ patient-derived samples (Fig. 4B). By hypothesizing that HIV can broadly affect $T_{FH}$ cells beyond the GC subset, we also analyzed other CD4$^+$ T cells positive for CXCR5 expression. Similar to the observation with GC $T_{FH}$ cells, CXCR5$^+$ memory CD4$^+$ T cells from patient samples occupied regions on the t-SNE map that overlapped with cells from HCs and additional areas that were unique (Fig. 4B). To delineate which $T_{FH}$ phenotypes were the dominant HIV-related features, we performed density-based local maxima cluster with support vector machine (DensVM) to automatically identify t-SNE clusters in an unbiased fashion (Fig. 4C and fig. S7) (*23*). We then generated a heatmap to visualize the staining intensity for individual markers and the relative contribution of HC- or HIV-derived cells to each cluster (Fig. 4D). This analysis revealed a high abundance of activated CD38$^+$ $T_{FH}$ cells in LN cells from HIV$^+$ individuals (clusters 1 and 2). CD38$^+$ $T_{FH}$ cells also colocalized with cells that expressed the highest levels of Ki67 and $T_{FH}$ markers PD-1, ICOS, B cell lymphoma 6 (BCL-6), and IL-21 on the t-SNE maps (fig. S8). Manual gating for CD38 on total CXCR5$^+$ memory CD4$^+$ T cell and GC $T_{FH}$ cells confirmed that $T_{FH}$ cells from HIV$^+$ patients were more highly activated compared with cells from HCs (Fig. 4E). A significantly higher proportion of CD38$^+$CXCR5$^+$ memory CD4$^+$ T cells stained for the GC marker CD57 and the expression of a CD38$^+$-activated phenotype additionally correlated with the capacity to produce IL-21 upon T cell stimulation (Fig. 4, F and G). Whereas LN location (cervical versus others) may contribute to some differences between cells from HIV$^+$ patients and HCs, changes in $T_{FH}$ cell phenotypes were also related to the severity of HIV infection in cells from the same site. For HIV-infected cervical LN samples,

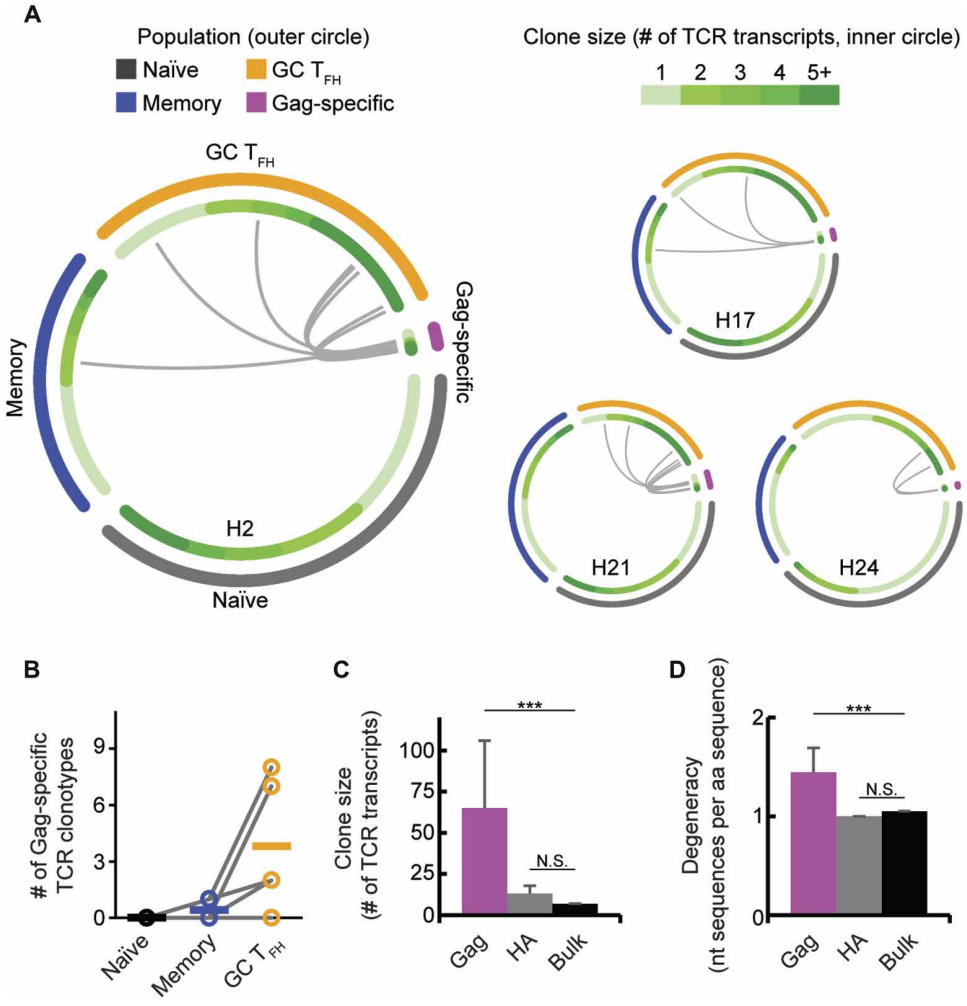


**Fig. 3. GC $T_{FH}$ cells exhibit HIV antigen–driven clonal expansion and selection.** (**A**) Gag-specific TCR clones overlap with HIV$^+$ LN CD4$^+$ T cell populations. Each thin slice of the arc represents a unique TCR sequence, ordered by the clone size (darker green for larger clones, inner circle). Gray curves indicate Gag-specific TCR nucleotide sequences found in naïve (gray, outer circle), memory (blue, outer circle), and GC $T_{FH}$ (orange, outer circle) populations. No Gag-overlapping clones were detected for one individual, H8 (not shown). (**B**) Number of Gag-specific TCR clones observed in naïve, memory, and GC $T_{FH}$ populations. Gray lines link the same patient. Bars indicate means (*P* values by two-tailed paired *t* test). (**C**) Mean clone size of Gag-specific T cells, HA-specific T cells, and bulk clones of unknown specificity from the GC $T_{FH}$ population. (**D**) Number of distinct nucleotide (nt) sequences per CDR3 amino acid (aa) sequence for Gag-specific T cells, HA-specific T cells, or bulk GC $T_{FH}$ cells. Data from all four individuals were aggregated for (C) and (D). Error bars indicate SEM. N.S., not significant. ***$P < 0.001$ by two-tailed *t* test.

high IL-21 expression in GC $T_{FH}$ cells correlated with peripheral CD4$^+$ T cell depletion by low CD4$^+$ T cell count (Fig. 4H). Other clinical features, including viral load or antiviral treatment at the time of LN excision, were not significantly associated with CD38 or IL-21 positivity in GC $T_{FH}$ cells (fig. S9). Collectively, high-dimensional $T_{FH}$ cell analyses identified an activation-related $T_{FH}$ cell signature in infected LNs characterized by an IL-21–dominant functional phenotype.

## Gag-reactive T cells preferentially express GC markers and produce IL-21 during chronic HIV infection

Because IL-21 plays a key role in B cell selection and differentiation, we further dissected the sequence repertoire, antigen specificity, and functional potential of IL-21–producing T cells. We adapted the method by Schultz *et al.* (*24*) and optimized cell capture using a streptavidin-based scaffold protein to couple anti–IL-21 antibodies onto the surface of memory T cells (fig. S10) (*25*). LN cells were incubated with IL-21 capturing complex and Gag peptides for 18 hours and then stained with an IL-21 detection antibody. Individually sorted single IL-21$^+$ T cells were processed for TCRβ chain amplification and sequencing (Fig. 5A) (*26*, *27*). In total, we analyzed TCR sequences from 185 Gag-reactive T cells in four untreated HIV$^+$ patients (table S6 and Fig. 5B). Clonally expanded T cells were detected in three of the four individuals. In samples where clonal expansion was observed, 3.6, 12.5, or 24.5% of Gag-reactive T cells express the exact same TCR sequence as that of another cell from the same person, with a single TCR clonotype occupying about a tenth of sequence repertoire from IL-21$^+$ T cells in two individuals (8.5 and 12.5%; Fig. 5B). These data provided a quantitation of clonotypic diversity of the T cell response to Gag peptides in HIV-infected LNs and demonstrated a highly restricted repertoire of IL-21–producing T cells in some HIV$^+$ patients.

Most of the IL-21$^+$ Gag-reactive T cells expressed a classic $T_{FH}$ cell phenotype, as indicated by high CXCR5, ICOS, and PD-1 expression (Fig. 5, C and D). These cells were also enriched for CD57 compared with bulk memory T cells in the same LN (Fig. 5, C and D). Although we did not detect a significant correlation between CD57 signal intensity and IL-21 frequency on CyTOF analyses (fig. S11), we additionally identified Gag-reactive T cells in a subset of donors using a cytokine-independent approach (*28*) and showed that Gag-reactive T cells identified by CD25 and OX40 up-regulation were also enriched for CD57 expression (Fig. 5, E and F). Together, these data indicate that T cell response to HIV antigens alters $T_{FH}$ cell phenotypes.

Because IL-21$^+$ GC $T_{FH}$ cells were most abundant in patients with more severe HIV infection, we hypothesized that HIV-specific T cells preferentially contributed to the increased IL-21 functional phenotype in the infected lymphoid environment. To test this idea, we compared IL-21 expression between Gag- and HA-reactive T cells from the same donor (fig. S12). LN-derived T cells specific for each antigen were identified by the CD25$^+$OX40$^+$ phenotype after peptide stimulation. IL-21–producing cells were measured as a subset of CD25$^+$OX40$^+$ $T_{FH}$ cells. Our data showed that significantly more Gag-reactive $T_{FH}$ cells produced IL-21 compared with HA-reactive T cells [average: 14.7% (Gag) versus 5.7% (HA); Fig. 5G]. As a percentage of GC $T_{FH}$ cells, Gag peptides also induced a larger IL-21 response compared with

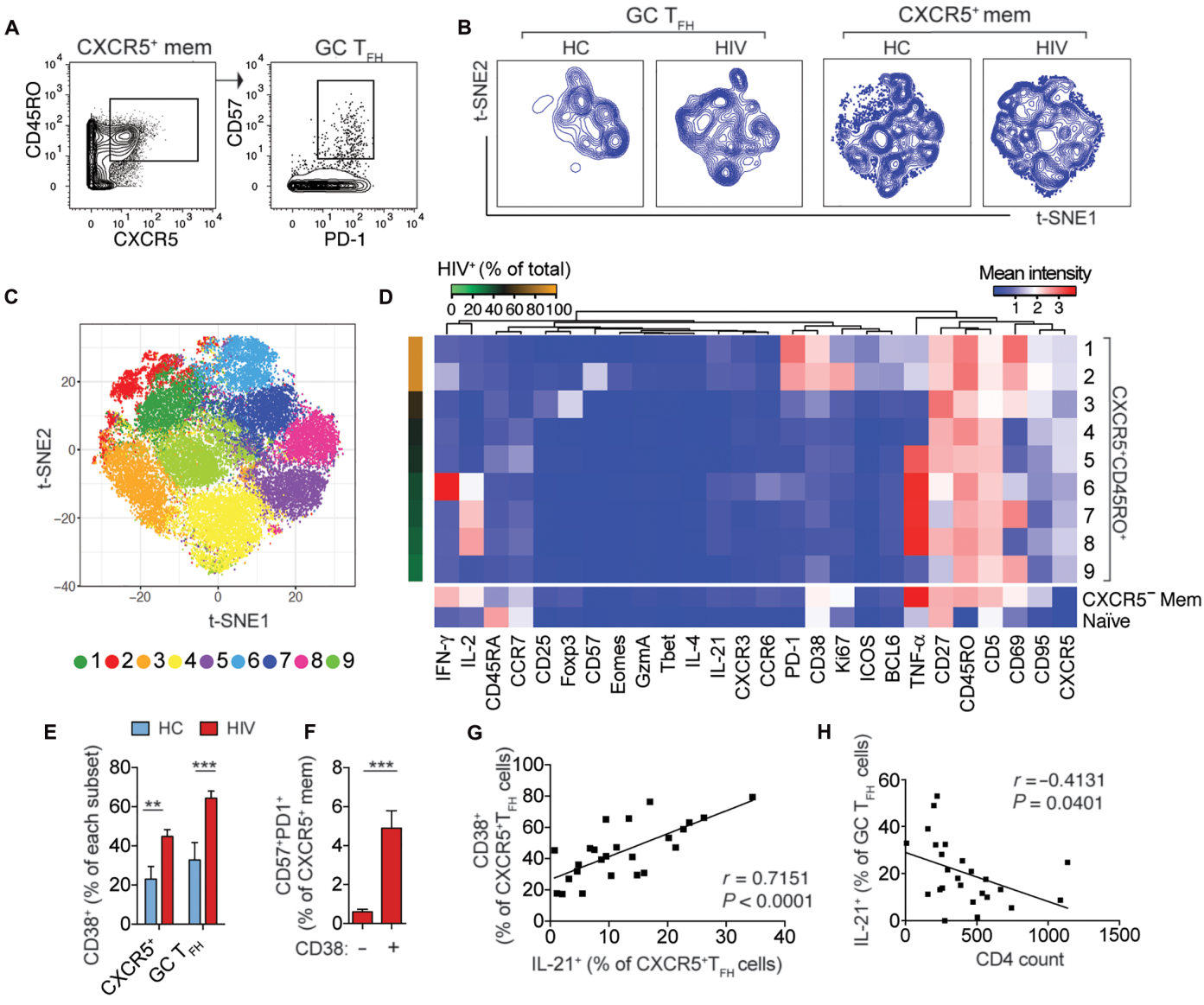


**Fig. 4. High-dimensional analysis of lymphoid CD4⁺ T cells identified distinct $T_{FH}$ cell subsets in HIV⁺ patients and HCs.** (**A**) Representative gates used to identify GC $T_{FH}$ cells for t-SNE analysis. (**B**) Contour plots were generated using FACS output files from Cytobank (GC $T_{FH}$ cells) or "cytofkit" package in R ($CXCR5^+CD45RO^+CD4^+$ T cells). Data include cells from 25 HIV⁺ patients and seven HCs. (**C**) Phenotypic clusters identified from $CXCR5^+$ memory $CD4^+$ T cells using DensVM. (**D**) Heatmap shows the average staining signal of indicated markers within each of the clusters identified in (C). Memory and naïve cells are shown at the bottom of the heatmap for comparison. Red-blue scale indicates staining intensity. Green-brown scale represents the relative frequency of HIV⁺ cells to total numbers of cells in each cluster. (**E**) Frequency of CD38 expression in $CXCR5^+$ $T_{FH}$ cells or GC $T_{FH}$ cells from HC ($n = 7$) or HIV⁺ ($n = 25$) patients. Data are mean ± SEM. $^{**}P < 0.005$ and $^{***}P < 0.0005$ by two-tailed $t$ test. (**F**) Frequency of $CD57^+PD1^+$ GC subset within $CD38^-$ or $CD38^+CXCR5^+$ $T_{FH}$ cells from HIV⁺ patients ($n = 25$). $^{***}P < 0.0005$ by paired two-tailed $t$ test. (**G**) Relationship between IL-21 expression and CD38 frequency in $CXCR5^+$ $T_{FH}$ cells. (**H**) Relationship between peripheral $CD4^+$ T cell count and IL-21⁺ GC $T_{FH}$ cells frequency. For (G) and (H), data are from 25 HIV⁺ patients; association was determined by Pearson correlation.

HA [average: 0.83% (Gag) versus 0.52% (HA); Fig. 5H]. Together, these data indicate that Gag-reactive T cells preferentially acquire a GC phenotype and produce IL-21 during chronic antigen stimulation in infected LNs.

### HIV infection is associated with less polyfunctional $T_{FH}$ cells

Although IL-21 is critical for $T_{FH}$ cell function, we also detected expression of other cytokines on CyTOF (Fig. 4D). These data are consistent with past analyses of pediatric tonsil cells, which revealed an abundance of cellular diversity within $T_{FH}$ cells that included effector-type $T_{FH}$ cells capable of producing different combinations of interferon-γ (IFN-γ), IL-2, tumor necrosis factor–α (TNF-α), or IL-17A (*29*). To better delineate the impact of HIV infection on the functional diversity of $T_{FH}$ cells, we performed manual gating to measure the frequency of $T_{FH}$ cells that produced IL-21, IFN-γ, TNF-α, IL-2, IL-4, and granzyme A. We restricted this part of the analyses to the GC subset using strictly defined $T_{FH}$ cell markers and used unstimulated cells to establish the baseline signal for each effector molecule in the absence

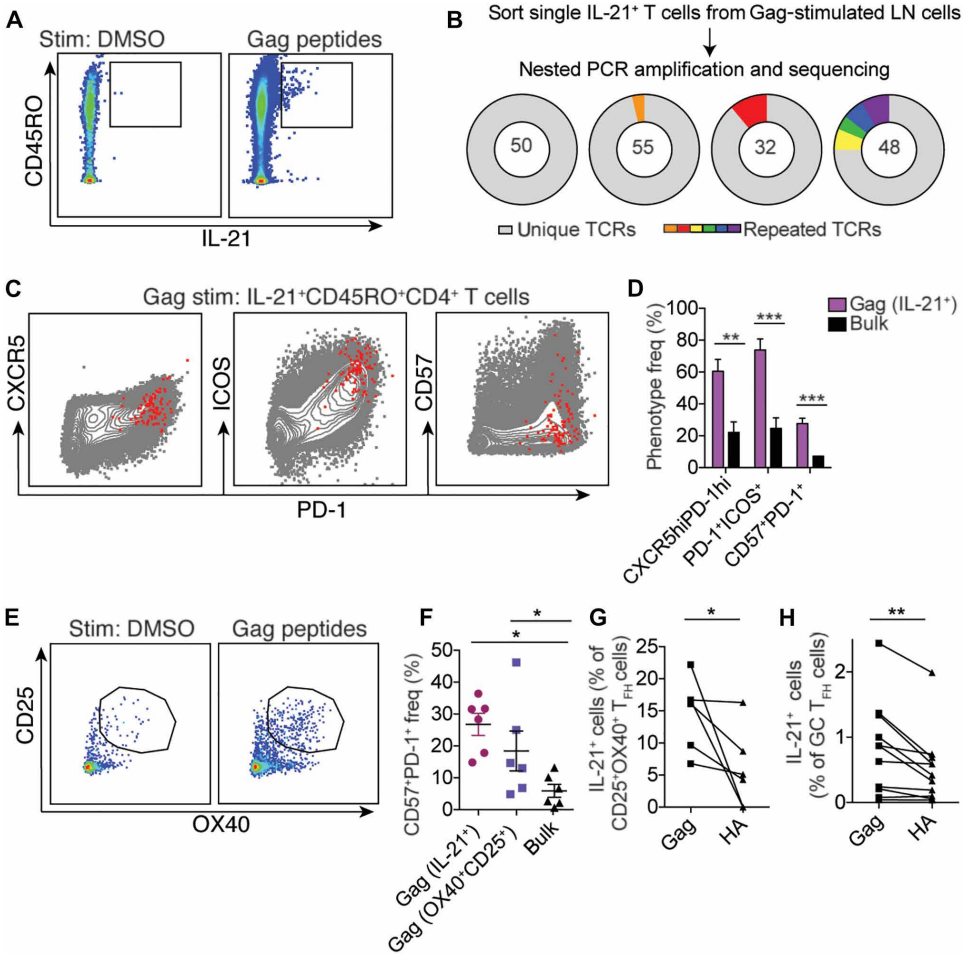


**Fig. 5. Gag-reactive $T_{FH}$ cells express IL-21 and acquire GC phenotype.** (**A**) Representative plots showing IL-21 staining used to identify Gag-reactive T cells. LN cells were stimulated for 18 hours with vehicle alone using dimethyl sulfoxide (DMSO) (left) or Gag peptides (right). (**B**) TCR sequencing of Gag-reactive IL-21$^+$ T cells. Each pie chart represents TCR sequences from one individual. Light gray color represents unique TCRs. Filled colors represent the fraction of cells expressing a TCR identical to that of another cell in each individual. The number of TCR sequences analyzed is indicated at the center of pie chart. (**C**) Phenotype of Gag-reactive IL-21$^+$ T cells (red) overlaid onto bulk CD4$^+$ T cells (gray). (**D**) Frequency of each indicated phenotypic subset within IL-21$^+$ Gag-reactive T cells or IL-21$^-$ bulk memory T cells from HIV$^+$ individuals ($n = 11$). $^{**}P < 0.005$ and $^{***}P < 0.0005$ by two-tailed $t$ test. (**E**) Representative plots showing identification of Gag-reactive T cells by CD25 and OX40 expression. (**F**) CD57$^+$PD-1$^+$ frequency of Gag-reactive T cells from HIV$^+$ individuals ($n = 6$) identified using IL-21 capture or by CD25 and OX40 up-regulation. (**G**) Frequency of CD25$^+$OX40$^+$CXCR5$^+$PD-1$^+$ $T_{FH}$ cells that coexpressed IL-21 after Gag or HA peptide stimulation from six HIV$^+$ individuals. (**H**) IL-21 expression within GC $T_{FH}$ subset in LN cells from 11 HIV$^+$ patients stimulated by Gag or HA peptides. The lines connect data from the same donor. For (F) to (H), $^*P < 0.05$ and $^{**}P < 0.005$ by paired two-tailed Wilcoxon signed-rank test.

of T cell activation (fig. S13). Our data showed positive staining for IFN-γ, TNF-α, IL-2, IL-4, and granzyme A in $T_{FH}$ cells, but $T_{FH}$ cells from HIV$^+$ patients secreted significantly less IFN-γ and granzyme A compared with HCs (Fig. 6A). Although not statistically significant, GC $T_{FH}$ cells from HIV$^+$ patients also secreted less TNF-α and had lower IL-2 production. To validate these observations, we used polychromatic flow cytometry to analyze a second set of samples that included eight new HIV$^+$ patients, five additional HCs, and two HCs analyzed previously by CyTOF. GC $T_{FH}$ cells defined using the same gating strategy by CXCR5, CD45RO, PD-1, and CD57 expression on CD4$^+$ T cells also showed an HIV-associated decrease in IFN-γ and granzyme A production (fig. S14). Collectively, our data revealed changes in $T_{FH}$ cell subsets that favor IL-21–producing populations in the setting of chronic antigen stimulation.

Because IL-21 and other effector molecules have not only overlapping but also distinct patterns of distribution on the t-SNE map (fig. S8B), we next asked how HIV affects the effector profile of IL-21$^+$ $T_{FH}$ cells. We used Boolean combination gates to create all possible combinations of IL-21 with other effector molecules stained by CyTOF (IFN-γ, TNF-α, IL-2, IL-4, and granzyme A). IL-21$^+$ cells were then grouped according to the number of additional effector molecules produced. Our data showed a decrease in polyfunctional IL-21$^+$ T cells that can produce multiple effector molecules in $T_{FH}$ cells from HIV$^+$ patients compared with HCs (fig. S15). Instead, more dedicated single IL-21–producing $T_{FH}$ cells were found in HIV$^+$ patients (Fig. 6B). To determine whether a similar type of IL-21$^+$ cells also circulated in the blood during chronic HIV infection, peripheral blood mononuclear cells (PBMCs) were obtained from a subset of HC and HIV$^+$ donors from whom we had paired LN samples. Circulating $T_{FH}$ cells ($cT_{FH}$) were identified as IL-21–producing CD4$^+$ T cells (*24*). We showed that, similar to cells in the LN, $cT_{FH}$ cells were more functionally focused on IL-21 expression in HIV$^+$ patients, and the abundance of IL-21 single-positive cells in the blood was highly correlated with the frequency of IL-21 single-positive $T_{FH}$ cells in the LNs (Fig. 6, B and C). Collectively, these data revealed an IL-21–dominant phenotype as a prevailing feature broadly shared by different types of $T_{FH}$ cells from HIV$^+$ patients.

Untreated HIV is associated with defective B cell differentiation. Past studies demonstrated that LNs from HIV$^+$ patients contain fewer memory B cells and more plasma cells (*3*, *4*), but how aberrant B cell subset distribution relates to changes in $T_{FH}$ cells remained unclear. By hypothesizing that IL-21–dominant $T_{FH}$ cells promote abnormal B cell development, we examined the relationship between the frequency of single IL-21$^+$ $T_{FH}$ cells and B cell phenotype. Memory B cells and plasma cells were identified using the same gating strategy as Perreau *et al.* (*3*) (Fig. 6D and fig. S16). We found that having a low frequency of isotype-switched memory B cells was associated with more single IL-21–producing cells (Fig. 6, E and G). A reciprocal relationship was observed for plasma cells, which was positively correlated with single IL-21–producing cells (Fig. 6, F and H). These data indicate that the accumulation of functionally focused IL-21$^+$ $T_{FH}$ cells is associated with lymphoid B cell pathology during HIV infection.

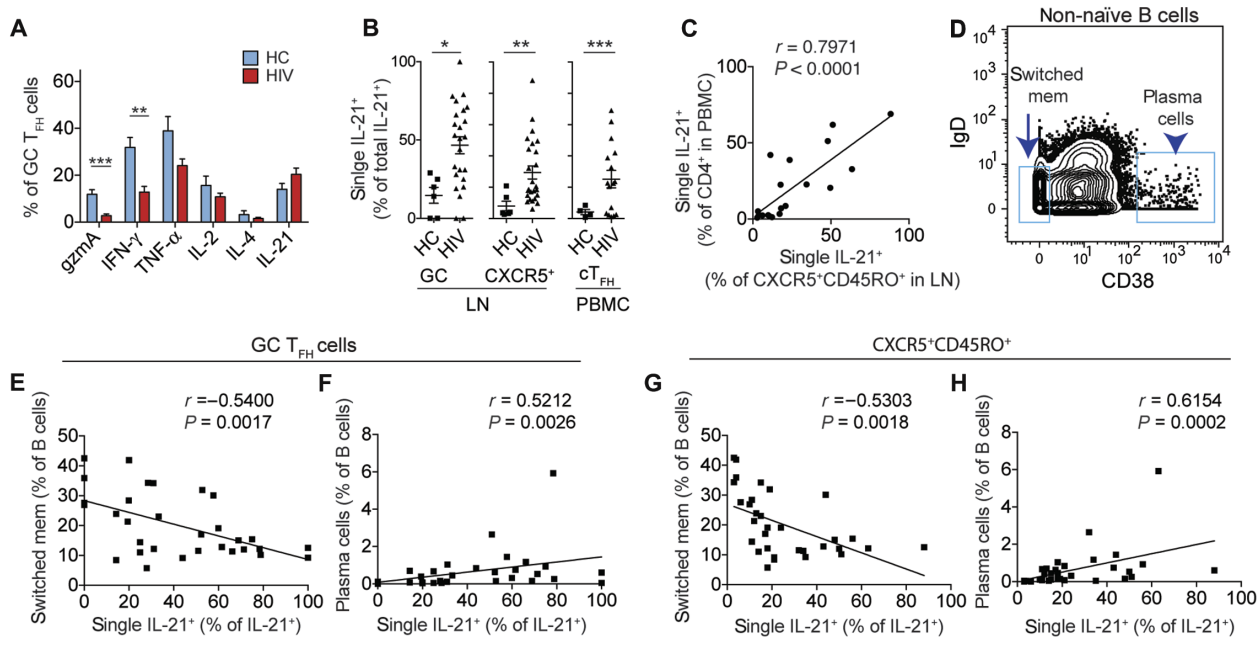


**Fig. 6. Dominant IL-21 expression in $T_{FH}$ cells correlate with B cell pathology in HIV-infected LNs.** (**A**) Frequency of GC $T_{FH}$ cells that positively stained for each indicated effector molecule as determined by CyTOF. $^{**}P < 0.005$ and $^{***}P < 0.0005$ by two-tailed *t* test ($n = 7$ HCs, 25 HIV$^+$ patients). (**B**) Bar graph showing the frequency of single IL-21–producing T cells as a percentage of total IL-21$^+$ T cells within each indicated $T_{FH}$ cell subset. $^*P < 0.05$, $^{**}P < 0.005$, and $^{***}P < 0.0005$ by two-tailed Wilcoxon signed-rank test (PBMCs: $n = 4$ HCs, 16 HIV$^+$ patients; LN: $n = 6$ HCs, 25 HIV$^+$ patients). (**C**) Plot shows the correlation between the abundance of single IL-21$^+$ T cells (as a percentage of total IL-21$^+$ T cells) in paired PBMCs and LNs from four HCs and 15 HIV$^+$ individuals. Association is determined by Pearson correlation. (**D**) IgD$^+$CD27$^-$ naïve B cells were excluded (also see fig. S16). Plots show gating strategy to identify switched memory B cells (IgD$^-$CD38$^-$) and plasma cells (IgD$^-$CD38$^{high}$) on non-naïve B cells. (**E** to **H**) Correlation between switched memory B cell and plasma cells with the abundance of single IL-21$^+$ T cells in GC $T_{FH}$ cells (E and F) or CXCR5$^+$CD45RO$^+$ CD4$^+$ T cells (G and H) ($n = 7$ HCs and 25 HIV$^+$ patients). Association was measured by Pearson correlation (E and G) or Spearman's rank correlation (F and H), depending on data normality as determined by D'Agostino-Pearson test.

## DISCUSSION

How HIV affects lymphoid $T_{FH}$ cells has been studied under limited settings. In part, the challenge has been the inaccessibility of human lymphoid tissues and the tools available to interrogate a small number of cells. Here, we overcame these challenges using LNs obtained for clinical diagnostics from a mostly untreated HIV$^+$ cohort. The data described here represent a comprehensive phenotype and TCR analysis of $T_{FH}$ cells in the LNs, including that of HIV-reactive T cells. We also analyzed LN samples from HIV$^-$ HCs, but because of ethical and practical limitations, HC-derived LNs were obtained from different body sites and should be interpreted with this potential caveat. Our data based on TCR repertoire sequencing analyses provided evidence for antigen-driven expansion of $T_{FH}$ cells and selection for certain preferred CDR3 sequences during chronic HIV infection. We further demonstrated that these GC $T_{FH}$ cells acquire a distinct functional phenotype and become dominated by an IL-21$^+$ functional subset.

The biological relevance for having different subsets of $T_{FH}$ cells is just now beginning to be understood. Using IL-21 and IL-4 reporter genes in mice to trace $T_{FH}$ cells that produce IL-21, IL-4, or both, Weinstein *et al.* (*30*) demonstrated temporal differences in the kinetics of IL-21 and IL-4 production and showed that IL-21$^+$, IL-21$^+$IL-4$^+$, and IL-4$^+$ $T_{FH}$ cells each provide specialized follicular helper function and support distinct aspects of B cell function and development. Here, we also detected various functional $T_{FH}$ cell subsets in healthy human LNs and showed that T cells identified using the classic $T_{FH}$ lineage markers have the potential to secrete many distinct types of effector molecules. Our data are consistent with the diversity of functional phenotypes previously observed in tonsils (*29*) and highlight the heterogeneity of $T_{FH}$ cells at a healthy baseline.

We used HIV infection to ask how prolonged antigen stimulation alters the composition of $T_{FH}$ cells in the LN. In vitro studies have suggested that $T_{FH}$ cells could become inhibited in the context of chronic inflammation and fail to activate appropriately to TCR stimulation via induction of PD-1–mediated inhibitory signals (*7*). The increase in $T_{FH}$ cells could then be explained by an overabundance of cytokine signals in HIV-infected LNs that activated T cells in an antigen-independent fashion (*12*, *13*). Although our data do not rule out a contribution from bystander T cell expansion, our data are most consistent with the model where $T_{FH}$ cell pathology, manifested as clonal expansion and reduced polyfunctionality, is primarily an antigen-driven process. By TCR repertoire sequencing, we showed that certain TCR clonotypes become expanded within GC $T_{FH}$ cells. A small portion of HIV-specific clones harbor distinct nucleotide sequences that converge to the same amino acid sequence—a signature of antigen-driven selection. Convergent selection of TCR sequences is expected only when there is external pressure to select for certain CDR3 binding motifs. These data provide strong evidence for an antigen-driven process and additionally suggest that B cells, in their capacity as antigen-presenting cells, also shape the composition of $T_{FH}$ cells. We measured the extent of clonal restriction by single-cell TCR sequencing. We found different clonal frequencies in Gag-reactive IL-21$^+$ T cells between different HIV$^+$ patients, with expanded clones occupying a significant proportion of Gag-reactive response in some individuals.

Although we did not evaluate Env-reactivity directly, reduced TCR diversity will likely also affect T cells that recognize other HIV antigens. How $T_{FH}$ cell repertoire relates to the selection of protective and/or neutralizing antibody responses remains poorly understood. The density of peptide–major histocompatibility complex (MHC) presented by competing B cells has been shown to be a major factor that determines the magnitude of T cell help (*31*–*33*), but the diversification of antigenic variants by viral mutation provides an additional layer of complexity in the selection of relevant B cells during chronic HIV infection (*34*). Previous studies have shown that early HIV Env gene diversity predicts development of antibody breadth (*35*). This raised the possibility that a diverse repertoire of HIV-specific $T_{FH}$ cells may be necessary to capture the breadth of viral variants, and an oligoclonal $T_{FH}$ population that focuses T cell reactivity to nonproductive but common antigenic viral sequences may neglect rare B cells that have neutralizing potential. Future studies to determine whether individuals with more diverse HIV-specific $T_{FH}$ cell repertoire are more successful at generating broadly neutralizing antibodies will provide additional insights.

One important open question is why an excess of expanded $T_{FH}$ cells in the LNs fails to provide superior B cell help during chronic HIV infection. Our data provided evidence that HIV infection alters the functional quality of $T_{FH}$ cells and shifts $T_{FH}$ cells toward an IL-21–dominant subset. In support of an antigen-dependent model of T cell activation, Gag-reactive T cells preferentially acquire GC features and secrete IL-21, indicating that HIV-reactive T cells directly contributed to altered $T_{FH}$ cell phenotype in infected LNs. In addition, because most of the GC $T_{FH}$ cells also acquire an altered phenotype, there are likely other secondary effects of HIV infection that extend beyond HIV-specific T cells. IL-$21^+$ $T_{FH}$ cells in HIV-infected LNs produce less of other types of cytokines. This IL-21–focused $T_{FH}$ cell subset could represent a more differentiated $T_{FH}$ cell population in response to persistent antigen stimulation. However, because having more IL-$21^+$ $T_{FH}$ cells in the LN was associated with severe HIV infection and aberrant B cell distribution, the accumulation of IL-$21^+$ $T_{FH}$ cells is likely counterproductive in the setting of HIV infection. The notion that an excess of the IL-21–producing subset could contribute to HIV-related B cell changes is consistent with previous studies in mice showing that IL-21 is required to maintain BCL-6 expression in B cells and promotes plasma cell differentiation (*30*, *36*, *37*). Changes in B cell subsets could also result from a relative decrease in other types of $T_{FH}$ cells, which would agree with recent studies that showed specialization of $T_{FH}$ cell subsets in regulating distinct aspects of B cell differentiation (*34*). Lastly, whether having a highly specialized population of clonally restricted $T_{FH}$ cells could divert T cell help to unprotective B cells remains to be determined.

We have defined the TCR and phenotypic repertoire of $T_{FH}$ cells during chronic HIV stimulation. Our work highlights an antigen-driven process that alters the composition of $T_{FH}$ cells in the lymphoid compartment. Collectively, our data suggest that, in addition to the size of the GC reaction, the functional profile and the compositional complexity of $T_{FH}$ cells are additional key measurements that could affect the quality of $T_{FH}$ cell responses to vaccines and infections.

## MATERIALS AND METHODS

### Study design

The goal of the study was to define $T_{FH}$ cell diversity in primary human LNs. All samples were de-identified and obtained with Institutional Review Board approval from the University of Pennsylvania. Participant characteristics are shown in table S5. Please see the Supplementary Materials for details on sample collection.

### CyTOF staining and data analyses

Cryopreserved cells were thawed and stained with a metal-conjugated antibody panel (table S4), after a 5-hour stimulation with PMA and ionomycin in the presence of monensin and brefeldin A. Antibody-stained cells were mixed with normalization beads and acquired on CyTOF 2. Bead standards were used to normalize CyTOF runs with the MATLAB-based normalizer (*22*). Data analyses were performed using Cytobank and "cytofkit" package in R. Please see the Supplementary Materials for detailed methods on cell staining and CyTOF analysis.

### TCRβ sequencing and analyses

TCR sequences from single cells were obtained by a series of three nested polymerase chain reactions, as previously described (*26*, *27*). TCR junctional region analysis was performed using IMGT/V-Quest. For bulk cell analyses, TCR library generation and raw sequence processing were performed using MIDs with primers listed in table S1 (*18*, *19*). Please see the Supplementary Materials for detailed methods on TCR sequencing.

### Statistical methods

Assessment of normality was performed using D'Agostino-Pearson test. Pearson or Spearman's rank correlation was used depending on the normality of the data to measure the degree of association. The best-fitting line was calculated using least-squares fit regression. Statistical comparisons were performed using two-tailed Student's *t* test or Wilcoxon signed-rank test, with a $P$ value of $<0.05$ as a cutoff to determine statistical significance. Multiple comparisons were corrected using Holm-Sidak method. Statistical analyses were performed using GraphPad Prism.

## SUPPLEMENTARY MATERIALS

immunology.sciencemag.org/cgi/content/full/3/22/eaan8884/DC1

Methods

Fig. S1. GC $T_{FH}$ cells are clonally expanded.

Fig. S2. Antigen-driven clonal selection signature in GC $T_{FH}$ cells of HIV-infected LNs.

Fig. S3. Identification of Gag- or HA-reactive T cells in cultured cells.

Fig. S4. HA-specific CD4 T cell clones detected in HIV-infected LNs.

Fig. S5. Batch normalization of CyTOF data using calibration beads.

Fig. S6. Identification of GC $T_{FH}$ cells from LN samples.

Fig. S7. High-dimensional analysis of $CXCR5^+CD45RO^+CD4^+$ T cells.

Fig. S8. Signal intensity of individual markers on t-SNE plots.

Fig. S9. Correlation between IL-21 frequency and CD38 expression with viral load and antiviral treatment.

Fig. S10. IL-21 surface capture effectively identified IL-21–producing T cells.

Fig. S11. Correlation between the frequency of IL-$21^+$ GC $T_{FH}$ cells and signal intensity of CD57 staining.

Fig. S12. $T_{FH}$ cells respond to Gag or HA peptides.

Fig. S13. Identification of effector molecule–producing $CD4^+$ T cells on CyTOF.

Fig. S14. Identification of effector molecule–producing $CD4^+$ T cells by flow cytometry.

Fig. S15. Frequency of IL-21–producing subsets in $T_{FH}$ cells in $HIV^+$ and HC samples.

Fig. S16. Identification of B cell subsets.

Table S1. TCRβ sequencing primers.

Table S2. TCR repertoire sequencing cell and transcript counts.

Table S3. Gag and HA TCR sequence reference panel.

Table S4. CyTOF antibody staining panel.

Table S5. Clinical characteristics and demographic information of LN samples.

Table S6. Gag-reactive TCR sequences from single-cell TCR sequencing of IL-$21^+$ cells.

Table S7. Tabulated raw data sets.

## REFERENCES AND NOTES


1. C. G. Vinuesa, M. A. Linterman, D. Yu, I. C. M. MacLennan, Follicular helper T cells. *Annu. Rev. Immunol.* **34**, 335–368 (2016).
2. S. Crotty, T follicular helper cell differentiation, function, and roles in disease. *Immunity* **41**, 529–542 (2014).
3. M. Perreau, A.-L. Savoye, E. De Crignis, J.-M. Corpataux, R. Cubas, E. K. Haddad, L. De Leval, C. Graziosi, G. Pantaleo, Follicular helper T cells serve as the major CD4 T cell compartment for HIV-1 infection, replication, and production. *J. Exp. Med.* **210**, 143–156 (2013).
4. M. Lindqvist, J. van Lunzen, D. Z. Soghoian, B. D. Kuhl, S. Ranasinghe, G. Kranias, M. D. Flanders, S. Cutler, N. Yudanin, M. I. Muller, I. Davis, D. Farber, P. Hartjen, F. Haag, G. Alter, J. Schulze zur Wiesch, H. Streeck, Expansion of HIV-specific T follicular helper cells in chronic HIV infection. *J. Clin. Invest.* **122**, 3271–3280 (2012).
5. N. F. Crum-Cianflone, E. Iverson, G. Defang, P. J. Blair, L. E. Eberly, J. Maguire, A. Ganesan, D. Faix, C. Duplessis, T. Lalani, T. Whitman, C. Brandt, G. Macalino, E. V. Millar, T. Burgess, Durability of antibody responses after receipt of the monovalent 2009 pandemic influenza A (H1N1) vaccine among HIV-infected and HIV-uninfected adults. *Vaccine* **29**, 3183–3191 (2011).
6. P. Tebas, I. Frank, M. Lewis, J. Quinn, L. Zifchak, A. Thomas, T. Kenney, R. Kappes, W. Wagner, K. Maffei, K. Sullivan; Center for AIDS Research and Clinical Trials Unit of the University of Pennsylvania, Poor immunogenicity of the H1N1 2009 vaccine in well controlled HIV-infected individuals. *AIDS* **24**, 2187–2192 (2010).
7. R. A. Cubas, J. C. Mudd, A.-L. Savoye, M. Perreau, J. van Grevenynghe, T. Metcalf, E. Connick, A. Meditz, G. J. Freeman, G. Abesada-Terk Jr., J. M. Jacobson, A. D. Brooks, S. Crotty, J. D. Estes, G. Pantaleo, M. M. Lederman, E. K. Haddad, Inadequate T follicular cell help impairs B cell immunity during HIV infection. *Nat. Med.* **19**, 494–499 (2013).
8. K. L. Boswell, R. Paris, E. Boritz, D. Ambrozak, T. Yamamoto, S. Darko, K. Wloka, A. Wheatley, S. Narpala, A. McDermott, M. Roederer, R. Haubrich, M. Connors, J. Ake, D. C. Douek, J. Kim, C. Petrovas, R. A. Koup, Loss of circulating CD4 T cells with B cell helper function during chronic HIV infection. *PLOS Pathog.* **10**, e1003853 (2014).
9. R. Cubas, J. van Grevenynghe, S. Wills, L. Kardava, B. H. Santich, C. M. Buckner, R. Muir, V. Tardif, C. Nichols, F. Procopio, Z. He, T. Metcalf, K. Ghneim, M. Locci, P. Ancuta, J.-P. Routy, L. Trautmann, Y. Li, A. B. McDermott, R. A. Koup, C. Petrovas, S. A. Migueles, M. Connors, G. D. Tomaras, S. Moir, S. Crotty, E. K. Haddad, Reversible reprogramming of circulating memory T follicular helper cell function during chronic HIV Infection. *J. Immunol.* **195**, 5625–5636 (2015).
10. S. L. Kohler, M. N. Pham, J. M. Folkvord, T. Arends, S. M. Miller, B. Miles, A. L. Meditz, M. McCarter, D. N. Levy, E. Connick, Germinal center T follicular helper cells are highly permissive to HIV-1 and alter their phenotype during virus replication. *J. Immunol.* **196**, 2711–2722 (2016).
11. F. T. Hufert, J. van Lunzen, G. Janossy, S. Bertram, J. Schmitz, O. Haller, P. Racz, D. von Laer, Germinal centre CD4+ T cells are an important site of HIV replication in vivo. *AIDS* **11**, 849–857 (1997).
12. A. Biancotto, J.-C. Grivel, S. J. Iglehart, C. Vanpouille, A. Lisco, S. F. Sieg, R. Debernardo, K. Garate, B. Rodriguez, L. B. Margolis, M. M. Lederman, Abnormal activation and cytokine spectra in lymph nodes of people chronically infected with HIV-1. *Blood* **109**, 4272–4279 (2007).
13. S.-A. Younes, M. L. Freeman, J. C. Mudd, C. L. Shive, A. Reynaldi, S. Panigrahi, J. D. Estes, C. Deleage, C. Lucero, J. Anderson, T. W. Schacker, M. P. Davenport, J. M. McCune, P. W. Hunt, S. A. Lee, S. Serrano-Villar, R. L. Debernardo, J. M. Jacobson, D. H. Canaday, R.-P. Sekaly, B. Rodriguez, S. F. Sieg, M. M. Lederman, IL-15 promotes activation and expansion of $CD8^+$ T cells in HIV-1 infection. *J. Clin. Invest.* **126**, 2745–2756 (2016).
14. G. Pizzolo, G. Semenzato, M. Chilosi, L. Morittu, A. Ambrosetti, N. Warner, M. Bofill, G. Janossy, Distribution and heterogeneity of cells detected by HNK-1 monoclonal antibody in blood and tissues in normal, reactive and neoplastic conditions. *Clin. Exp. Immunol.* **57**, 195–206 (1984).
15. M. B. Bowen, A. W. Butch, C. A. Parvin, A. Levine, M. H. Nahm, Germinal center T cells are distinct helper-inducer T cells. *Hum. Immunol.* **31**, 67–75 (1991).
16. C. H. Kim, L. S. Rott, I. Clark-Lewis, D. J. Campbell, L. Wu, E. C. Butcher, Subspecialization of $CXCR5^+$ T cells: B helper activity is focused in a germinal center–localized subset of $CXCR5^+$ T cells. *J. Exp. Med.* **193**, 1373–1381 (2001).
17. J. R. Kim, H. W. Lim, S. G. Kang, P. Hillsamer, C. H. Kim, Human $CD57^+$ germinal center-T cells are the major helpers for GC-B cells and induce class switch recombination. *BMC Immunol.* **6**, 3 (2005).
18. B. S. Wendel, C. He, M. Qu, D. Wu, S. M. Hernandez, K.-Y. Ma, E. W. Liu, J. Xiao, P. D. Crompton, S. K. Pierce, P. Ren, K. Chen, N. Jiang, Accurate immune repertoire sequencing reveals malaria infection driven antibody lineage diversification in young children. *Nat. Commun.* **8**, 531 (2017).
19. K.-Y. Ma, C. He, B. S. Wendel, C. M. Williams, J. Xiao, H. Yang, N. Jiang, Immune repertoire sequencing using molecular identifiers enables accurate clonality discovery and clone size quantification. *Front. Immunol.* **9**, 33 (2018).
20. Q. Jia, J. Zhou, G. Chen, Y. Shi, H. Yu, P. Guan, R. Lin, N. Jiang, P. Yu, Q.-J. Li, Y. Wan, Diversity index of mucosal resident T lymphocyte repertoire predicts clinical prognosis in gastric cancer. *Oncoimmunology* **4**, e1001230 (2015).
21. J. Lin, Divergence measures based on the Shannon entropy. *IEEE Trans. Inf. Theory* **37**, 145–151 (1991).
22. R. Finck, E. F. Simonds, A. Jager, S. Krishnaswamy, K. Sachs, W. Fantl, D. Pe'er, G. P. Nolan, S. C. Bendall, Normalization of mass cytometry data with bead standards. *Cytometry A* **83**, 483–494 (2013).
23. K. Shekhar, P. Brodin, M. M. Davis, A. K. Chakraborty, Automatic Classification of Cellular Expression by Nonlinear Stochastic Embedding (ACCENSE). *Proc. Natl. Acad. Sci. U.S.A.* **111**, 202–207 (2014).
24. B. T. Schultz, J. E. Teigler, F. Pissani, A. F. Oster, G. Kranias, G. Alter, M. Marovich, M. A. Eller, U. Dittmer, M. L. Robb, J. H. Kim, N. L. Michael, D. Bolton, H. Streeck, Circulating HIV-specific interleukin-$21^+CD4^+$ T cells represent peripheral Tfh cells with antigen-dependent helper functions. *Immunity* **44**, 167–178 (2016).
25. J. Huang, X. Zeng, N. Sigal, P. J. Lund, L. F. Su, H. Huang, Y.-h. Chien, M. M. Davis, Detection, phenotyping, and quantification of antigen-specific T cells using a peptide-MHC dodecamer. *Proc. Natl. Acad. Sci. U.S.A.* **113**, E1890–E1897 (2016).
26. L. F. Su, B. A. Kidd, A. Han, J. J. Kotzin, M. M. Davis, Virus-specific $CD4^+$ memory-phenotype T cells are abundant in unexposed adults. *Immunity* **38**, 373–383 (2013).
27. A. Han, J. Glanville, L. Hansmann, M. M. Davis, Linking T-cell receptor sequence to functional phenotype at the single-cell level. *Nat. Biotechnol.* **32**, 684–692 (2014).
28. J. M. Dan, C. S. Lindestam Arlehamn, D. Weiskopf, R. da Silva Antunes, C. Havenar-Daughton, S. M. Reiss, M. Brigger, M. Bothwell, A. Sette, S. Crotty, A cytokine-independent approach to identify antigen-specific human germinal center T follicular helper cells and rare antigen-specific $CD4^+$ T cells in blood. *J. Immunol.* **197**, 983–993 (2016).
29. M. T. Wong, J. Chen, S. Narayanan, W. Lin, R. Anicete, H. T. Kiaang, M. A. C. De Lafaille, M. Poidinger, E. W. Newell, Mapping the diversity of follicular helper T cells in human blood and tonsils using high-dimensional mass cytometry analysis. *Cell Rep.* **11**, 1822–1833 (2015).
30. J. S. Weinstein, E. I. Herman, B. Lainez, P. Licona-Limón, E. Esplugues, R. Flavell, J. Craft, $T_{FH}$ cells progressively differentiate to regulate the germinal center response. *Nat. Immunol.* **17**, 1197–1205 (2016).
31. G. D. Victora, T. A. Schwickert, D. R. Fooksman, A. O. Kamphorst, M. Meyer-Hermann, M. L. Dustin, M. C. Nussenzweig, Germinal center dynamics revealed by multiphoton microscopy with a photoactivatable fluorescent reporter. *Cell* **143**, 592–605 (2010).
32. G. D. Victora, M. C. Nussenzweig, Germinal centers. *Annu. Rev. Immunol.* **30**, 429–457 (2012).
33. D. Depoil, R. Zaru, M. Guiraud, A. Chauveau, J. Harriague, G. Bismuth, C. Utzny, S. Müller, S. Valitutti, Immunological synapses are versatile structures enabling selective T cell polarization. *Immunity* **22**, 185–194 (2005).
34. J. M. Cuevas, R. Geller, R. Garijo, J. López-Aldeguer, R. Sanjuán, Extremely high mutation rate of HIV-1 in vivo. *PLOS Biol.* **13**, e1002251 (2015).
35. A. Piantadosi, D. Panteleeff, C. A. Blish, J. M. Baeten, W. Jaoko, R. S. McClelland, J. Overbaugh, Breadth of neutralizing antibody response to human immunodeficiency virus type 1 is affected by factors early in infection but does not influence disease progression. *J. Virol.* **83**, 10269–10274 (2009).
36. D. Zotos, J. M. Coquet, Y. Zhang, A. Light, K. D'Costa, A. Kallies, L. M. Corcoran, D. I. Godfrey, K.-M. Toellner, M. J. Smyth, S. L. Nutt, D. M. Tarlinton, IL-21 regulates germinal center B cell differentiation and proliferation through a B cell–intrinsic mechanism. *J. Exp. Med.* **207**, 365–378 (2010).
37. R. Ettinger, G. P. Sims, A.-M. Fairhurst, R. Robbins, Y. S. da Silva, R. Spolski, W. J. Leonard, P. E. Lipsky, IL-21 induces differentiation of human naive and memory B cells into antibody-secreting plasma cells. *J. Immunol.* **175**, 7867–7879 (2005).


**Acknowledgments:** We thank J. Wherry, R. Herati, B. Bengsch, and C. Blish for helpful discussions. We would like to thank J. Podnar and M. Wilson for helping with the sequencing runs. HIV-1 Con B Gag Peptide Set was obtained through the NIH AIDS Reagent Program, Division of AIDS, NIAID, NIH. **Funding:** L.F.S., D.d.A., and B.A. were supported by Medical Research Grant from W. W. Smith Charitable Trust Foundation, Penn Center for AIDS Research Pilot and Feasibility grant (P30-AI045008), the Veterans Affairs Merit Award (IMMA-020-15F), and NIH National Institute of Allergy and Infectious Diseases (R01AI134879). N.J., B.S.W., S.M.H., and K.-Y.M. were supported by NIH grants R00AG040149 (to N.J.), S10OD020072 (to N.J.), and the Welch Foundation grant F1785 (to N.J.). N.J. is a Cancer Prevention and Research Institute of Texas Scholar and a Damon Runyon-Rachleff Innovator. B.S.W. is a recipient of the Thrust 2000–George Sawyer Endowed Graduate Fellowship in Engineering. **Author contributions:** L.F.S. and N.J. designed the study. B.S.W. performed bulk TCR sequencing and data analysis. C.H. analyzed TCR sequencing data. D.d.A. performed CyTOF and IL-21

capture experiments. B.A. performed in vitro peptide stimulation and single-cell TCR sequencing. P.M.D.R.-E., Y.A.-T., and G.R.-T. established the infrastructure for HIV$^+$ patient recruitment and provided LN samples and the associated clinical information. S.M.H. assisted with TCR sequencing library preparation. K.-Y.M. adapted the TCR repertoire sequencing protocol. M.R.B. contributed to the LNs from healthy individuals. J.H. and L.P. prepared tetrameric scaffold protein. P.A.G. provided statistical support. L.F.S., N.J., and B.S.W. wrote and edited the paper. **Competing interests:** N.J. is a scientific adviser of ImmuDX LLC. The other authors declare that they have no competing financial interests. **Data and materials availability:** The data for this study have been deposited in the database of Genotypes and Phenotypes under the accession number phs001548.v1.p1.

Submitted 5 June 2017
Resubmitted 29 November 2017
Accepted 16 February 2018
Published 6 April 2018
10.1126/sciimmunol.aan8884

**Citation:** B. S. Wendel, D. del Alcazar, C. He, P. M. Del Río-Estrada, B. Aiamkitsumrit, Y. Ablanedo-Terrazas, S. M. Hernandez, K.-Y. Ma, M. R. Betts, L. Pulido, J. Huang, P. A. Gimotty, G. Reyes-Terán, N. Jiang, L. F. Su, The receptor repertoire and functional profile of follicular T cells in HIV-infected lymph nodes. *Sci. Immunol.* **3**, eaan8884 (2018).

Science Immunology

# The receptor repertoire and functional profile of follicular T cells in HIV-infected lymph nodes

Ben S. Wendel, Daniel del Alcazar, Chenfeng He, Perla M. Del Río-Estrada, Benjamas Aiamkitsumrit, Yuria Ablanedo-Terrazas, Stefany M. Hernandez, Ke-Yue Ma, Michael R. Betts, Laura Pulido, Jun Huang, Phyllis A. Gimotty, Gustavo Reyes-Terán, Ning Jiang and Laura F. Su

*Sci. Immunol.* **3**, eaan8884.
DOI: 10.1126/sciimmunol.aan8884

**Zooming in on human lymph nodes**

Follicular helper T cells ($T_{FH}$) play an essential role in shaping B cell–mediated antibody responses. By obtaining lymph nodes from HIV $^{+}$ individuals, Wendel *et al*. have used mass cytometry and TCR sequencing to directly examine the $T_{FH}$ response to HIV. They report that HIV infection alters the clonality of $T_{FH}$ cells with severe infections resulting in pronounced oligoclonal $T_{FH}$ responses. From a functional standpoint, they found that $T_{FH}$ cells in the lymph nodes of HIV $^{+}$ individuals secreted interleukin-21 but were less polyfunctional as compared with $T_{FH}$ cells from healthy individuals and that this lack of polyfunctionality correlated with impaired isotype switching of B cells in the lymph nodes.